Ultra-dense energy storage utilizing high melting point metallic alloys and photovoltaic cells

Alejandro Datas, Antonio Martí, Carlos del Cañizo and Antonio Luque

***Abstract* — A novel concept for energy storage utilizing high melting point metallic alloys and photovoltaic cells is presented. In the proposed system, the energy is stored in the form of latent heat of metallic alloys and converted to electricity upon demand by infrared sensitive photovoltaic cells. Silicon is considered in this paper due to its extremely high latent heat (1800 J/g), melting point (1410ºC), low cost (~$1.7/kg) and abundance on earth. The proposed solution enables an enormous energy storage density of ~ 500 Wh/kg and ~ 1 MWh/m^3, which is 12 times higher than that of lead-acid batteries, 4 times than that of Li-ion batteries and 10 to 20 times than that of the molten salts utilized in CSP systems.**

***Index Terms* — energy storage, thermophotovoltaics, metallic alloys, silicon, phase change materials.**

I. Introduction

Developing novel energy storage (ES) technologies at competitive cost and utilizing abundant materials is essential in order to manage a future electric system based on renewables. Today's global ES capacity is less than 3% of the installed power capacity and 95% of this capacity is provided by pumped hydroelectric systems [1], which is restricted to locations with very particular characteristics. The global demand of advanced ES systems (both heat and electricity) is expected to grow to 32,000 TWh by 2035, a 70% increase from 2012. Specifically, more than 6,000 GW of new global electricity storage capacity is expected to be required by 2030 [2].

Nowadays, there is no definitive ES solution. In the field of electricity storage, some of the existing technologies (e.g. batteries) are affected by scarcity and supply risk of relevant materials such as lithium, cobalt, tantalum or rare earths [1]. Some others must solve serious security issues (e.g. hydrogen and NaS batteries). In the field of thermal energy storage (TES) for power generation the existing technologies (most of them based on molten salts) are either inefficient or have a high cost [3].

In this paper we describe a novel ES concept for both heat and electricity that has the potential to achieve one of the highest energy densities among the existing ES solutions and uses abundant and safe materials. This system utilizes metallic alloy phase change materials (PCM) for TES and infrared-sensitive photovoltaic cells, from now on thermophotovoltaic (TPV) cells, for power generation.

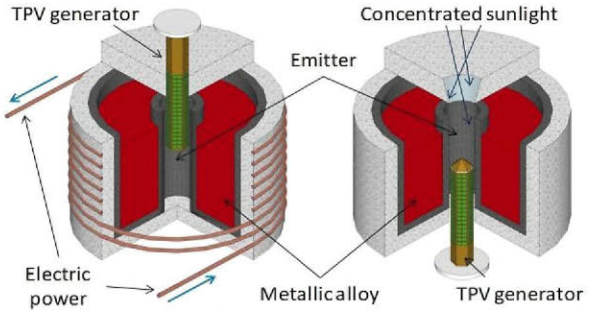

Fig. 1. Electric-ES (left) and solar-ES (right) systems utilizing high melting point metallic alloys and thermo-photovoltaic (TPV) cells for electricity production [4].

II. System Description

Fig.1 shows two possible configurations of the ES system [4]: electric and solar. In the first case a highly electrically conductive solenoid surrounds the vessel containing a metallic alloy. When alternating current passes through the solenoid, the oscillating magnetic field that is created within the alloy generates the so-called eddy currents. These currents heat up the metallic alloy by Joule effect until melting. As a result, electrical energy is stored in the form of the latent heat within the alloy. In the second case, concentrated solar power heats the inner walls of the vessel containing the alloy. If the sunlight concentration factor is high enough [5], [6] (above 1000 suns) the solar heat will produce the melting of the alloy and consequently, solar energy will be stored as latent heat within the alloy. Other arrangements not illustrated in this paper may use the waste heat from high temperature industrial processes.

In both cases of Fig.1 the stored heat is released in the form of electricity by using a TPV converter, which comprises a number of infrared sensitive photovoltaic cells that directly produce electricity from radiant heat. In contrast to conventional heat engines, the contact-less nature of TPV converters enable extremely high temperature operation, which is essential for this kind of systems. Besides, TPV can provide extremely high power densities (power-to-weight and power-to-volume ratio) at low maintenance costs (neither moving parts nor working fluids within the converter) along with silent operation, which is important for decentralized ES applications. Furthermore, the TPV conversion efficiency is

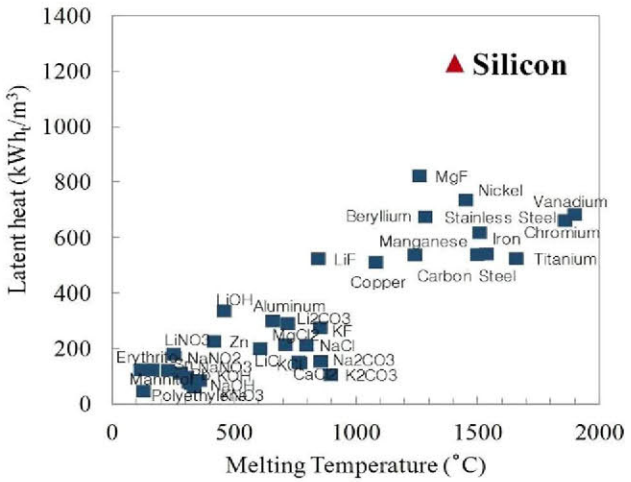

Fig. 2. Latent heat of fusion of different materials as a function of the melting temperature.

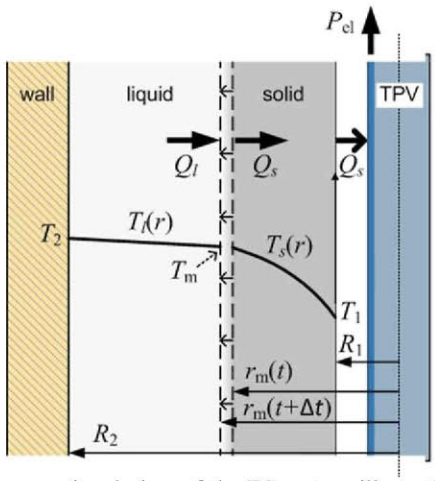

Fig. 3. Cross-sectional view of the ES system illustrating the heat transfer from the liquid PCM to the TPV converter and the resultant temperature distribution.

very high, potentially exceeding 50% due to the possibility of sub-bandgap photon recycling, which can be accomplished, for instance, by using reflectors in the back side of the TPV cells [7].

When electricity is demanded from the ES system, the TPV generator is moved in the cylindrical cavity formed by the inner walls of the vessel, from now-on referred to as emitter (Fig.1). Then, the TPV converter is irradiated by the emitter (which is in direct contact with the molten alloy) and produces electricity. During this process, the alloy progressively solidifies creating a crust of solid alloy around the emitter. This crust difficults the flow of heat from the liquid alloy to the emitter. However, the high solid-phase thermal conductivity of metallic alloys enormously mitigates the impact of this effect on the output system power.

Notice that these systems have the possibility of delivering not only electricity, but also heat from the TPV cells cooling, which might be beneficial in some particular applications such as in domestic heating, where the output coolant temperatures of 40-70°C match perfectly with the heating temperature requirements.

From the previous description, it is evident that the energy density (stored energy per unit of volume or weight) of these systems relies on the latent heat of the metallic alloy. Besides, the alloy's melting temperature determines the TPV conversion efficiency and power density (W/cm^2). Thus, high melting point and high latent heat are desirable properties for the metallic alloy. Among all the possible candidates, silicon stands out as the most promising one [6], due to its high latent heat of 1800 J/g, melting temperature of 1410°C (see Fig.2), very low cost of $1.7/kg, and the great abundance on earth. Thus, in this paper we analyze the case in which pure silicon is used. The analysis of other promising alloys will be presented in future works.

II. SYSTEM MODEL

In order to describe the transient performance of the ES system, we have assumed a quasi-1D analytical model in which the solid-liquid interface is a moving cylinder at a distance $r_m(t)$ from the axial center of the system (Fig.3). To solve the problem we followed the quasi-stationary approach used in [8] assuming an adiabatic (loss-less) container and neglecting natural convection in the liquid. Due to the later assumption the 1D-Fourier conduction law applies to describe the heat flow in both liquid and solid phases:

$$Q_{l,s} = 2\pi r L k_{l,s} \frac{dT}{dr} \tag{1}$$

By integrating (1) in the solid and liquid we obtain the following expressions for the temperatures T_1 (r=R_1) and T_2 (r=R_2) as a function of the melting temperature (T_m)

$$T_1 = T_m - \frac{Q_s}{2\pi L k_s} \ln\left|\frac{r_m(t)}{R_1}\right| \tag{2}$$

$$T_2 = T_m + \frac{Q_l}{2\pi L k_l} \ln\left|\frac{R_2}{r_m(t)}\right| \tag{3}$$

where k_s and k_l are the thermal conductivities of the solid and liquid PCM, respectively. Due to the assumption of adiabatic container, the difference between the energy transferred from the liquid to the solid equals the energy employed in performing the phase change of a the PCM contained in between $r_m(t)$ and $r_m(t+\Delta t)$, which leads to:

$$\begin{aligned}&(Q_l - Q_s)\Delta t = \\ &= 2\pi L L_f \rho_l r_m(t)\left(r_m(t+\Delta t) - r_m(t)\right)\end{aligned} \tag{4}$$

TABLE I

SILICON THERMAL PROPERTIES

property	sym	value
Latent heat of fusion	L_f	1800 J/g
Thermal conductivity (solid)	k_s	25 W/m-K
Thermal conductivity (liquid)	k_l	50 W/m-K
Density (solid & liquid)	$\rho_l=\rho_s$	2520 kg/m^3
Heat capacity (solid & liquid)	$c_{ps}=c_{pl}$	1040 J/kg-K
Melting point	T_m	1680 K

TABLE II

OTHER SYSTEM PARAMETERS

property	sym	value
TPV cell bandgap	ε_G	0.5 eV
TPV cell BSR reflectivity	ρ_{BR}	sweep param
TPV cell temperature	T_c	300 K
TPV cell voltage	V	optimized
PCM length	L	sweep param
PCM inner radius	R_1	sweep param
PCM outer radius	R_2	sweep param

where L_f and ρ_l are the latent heat of fusion and the density of the liquid PCM, respectively. An additional equation is obtained analyzing the radiative exchange between the emitter surface ($r=R_1$) and the TPV converter. This analysis has already been done in [7] and results in the following equation

$$Q_s/\pi = -\dot{E}(0,\infty,T_1,qV) + F_{ec}\dot{E}(\varepsilon_G,\infty,T_c,qV) + \frac{\rho_{BR}F_{ec}}{1-\rho_{BR}}\dot{E}(0,\infty,T_1,qV) \quad (5)$$

where

$$\dot{E}(\varepsilon_1,\varepsilon_2,T,\mu) = \frac{2}{h^3c^2}\int_{\varepsilon_1}^{\varepsilon_2}\frac{\varepsilon^3 d\varepsilon}{\exp[(\varepsilon-\mu)/kT]-1} \quad (6)$$

is the radiative energy flux emitted by a surface at temperature T and with chemical potential μ in vacuum, in the spectral interval (ε_1, ε_2), in the normal direction and per unit of solid angle. Equation (5) is valid under the assumption of sharp cut-off TPV cell absorptivity (from 100% to 0%) at the bandgap edge (ε_G) and assumes a reflector of reflectivity ρ_{BR} located on the back side of the TPV cells. V is the voltage of the TPV cells and $F_{ec}=A_c/A_1$ is the emitter-to-cell view factor, which can be approximated to the ratio of the cells area (A_c) to the emitter area (A_1).

Finally, due to adiabatic container the total energy stored in the PCM is delivered only by heat radiation through the emitter surface, which leads to

$$E_{tot}(t+\Delta t) = E_{tot}(t) - Q_s\Delta t \quad (7)$$

where E_{tot} is the total thermal energy stored in the PCM including both specific and latent heat:

$$E_{tot}/(2\pi L) = \rho_s c_{ps}\int_{R_1}^{r_m} rT_s(r)dr + \rho_l c_{pl}\int_{r_m}^{R_2} rT_l(r)dr + \rho_l L_f(R_2^2-r_m^2)/2 \quad (8)$$

Integrals in (8) can be analytically solved by introducing the expressions for $T_s(r)$ and $T_l(r)$ obtained from the integration in (1):

$$\int_{R_1}^{r_m} rT_s(r)dr = \frac{1}{2}\left(r_m^2T_m - R_1^2T_1 - \frac{Q_s}{4\pi Lk_s}\left(r_m^2-R_1^2\right)\right) \quad (9)$$

$$\int_{r_m}^{R_2} rT_l(r)dr = \frac{1}{2}\left[R_2^2T_2 - r_m^2T_m - \frac{Q_l}{2\pi Lk_l}\left(r_m^2-R_2^2\right)\cdot\left(2\ln|r_m|-0.5\right)\right] \quad (10)$$

The equations (2-5) and (7) can be solved numerically to obtain T_1, T_2, Q_l, Q_s and $r_m(t+\Delta t)$. Finally, assuming that the TPV cells have only radiative recombination, the output power from the TPV converter is given by [7]

$$P_{el} = \pi A_c qV\times\dot{N}(\varepsilon_G,\infty,T_1,0) - (1+n_s^2(1-\rho_{BR}))\dot{N}(\varepsilon_G,\infty,T_c,qV) \quad (11)$$

where

$$\dot{N}(\varepsilon_1,\varepsilon_2,T,\mu) = \frac{2}{h^3c^2}\int_{\varepsilon_1}^{\varepsilon_2}\frac{\varepsilon^2 d\varepsilon}{\exp[(\varepsilon-\mu)/kT]-1} \quad (12)$$

has the same meaning than $\dot{E}$ but for the photon flux instead of the energy flux.

IV. SYSTEM PERFORMANCE

Equations (2-5) and (7) are solved for the silicon parameters listed in Table I. The TPV cells are assumed to be ideal (only radiative recombination) with a bandgap of 0.5eV, which could be manufactured for instance using InGaAsSb alloys on GaSb substrates.

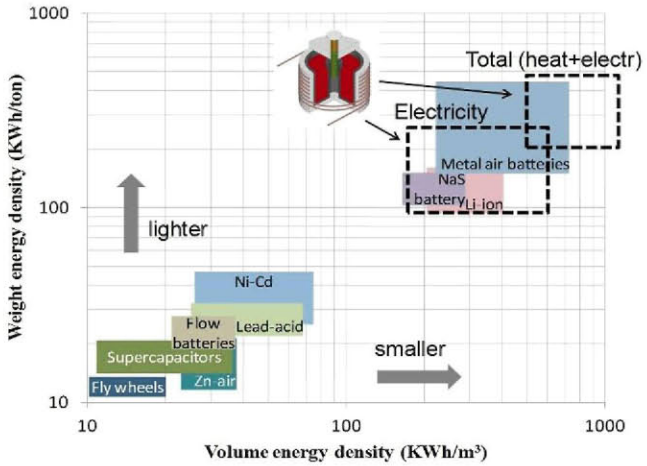

Fig. 4. Energy density of several electricity storage systems compared with that of the proposed ES system (from several sources)

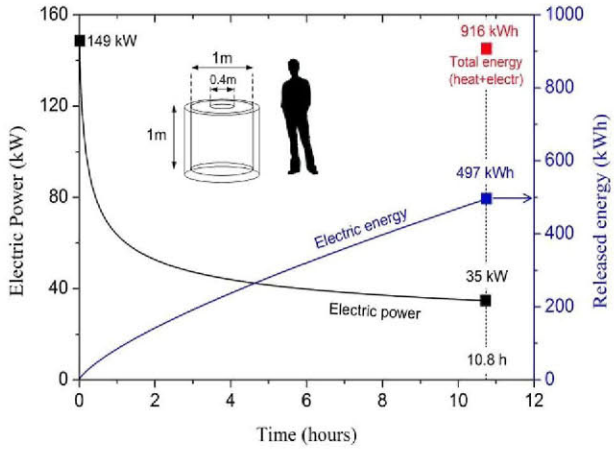

Fig. 5. Output power as a function of time during the discharge of an ES system (L=1m, R_1=0.2m, R_2=0.5m and ideal 0.5eV TPV cells). This result represents the full-power discharge mode, i.e. the TPV converter is entirely introduced in the cavity from the beginning.

Table III shows the model results for the discharge of the ES system with different geometries. Initial condition is that emitter temperature equals the silicon's melting point, so that energy is released from the system during the silicon solidification. The system is considered discharged when all silicon is solidified. Notice that the values in Table III refer to the full-power discharge mode, i.e. when the TPV converter is entirely introduced in the cavity from the beginning, which provides the highest power-to-discharge time ratio.

From Table III we conclude that total energy densities (heat plus electricity) of ~ 1 MW/m^3 and electric energy densities of ~500 kWh/m^3 are attainable, which is about 4-times (if total energy is accounted) higher than that of Li-ion batteries (Fig.4). Besides, the proposed ES system is fully scalable in terms of power (from kW to MW), energy (from tens of kWh to tens of MWh) and discharge time (hours to days).

Fig.5 shows the output power as a function of time for the case of an ES system with L = 1 m, R_1 = 0.2 m and R_2 = 0.5 m. This particular arrangement provides enough energy (heat plus electricity) to power 32 Spanish homes (average consumption of 10,500 kWh/home-year) during 24 hours. Smaller systems (microwave oven size) could be scaled to power one single home during one full day (see Table III).

Another interesting feature of these systems is the very high power peak at the start of the discharge (Fig.5) in the full-

TABLE III

ENERGY STORAGE SYSTEM OUTPUT CHARACTERISTICS

TPV converter (0.5eV)	Size (*) (m)			Released Energy (kWh)		Energy density (**) (kWh/m^3)			Output Electrical Power (kW)			Discharge time (***) (hours)
	L	R_1	R_2	Heat	Electricity	Total	Heat	Electricity	Peak	Average	Minimum	
Ideal (loss-less)	0.4	0.04	0.2	28.8	34.6	557.7	254.7	302.9	12.0	5.9	5.1	5.8
	0.4	0.02	0.2	29.3	34.8	567.3	259.2	308.1	6.0	3.3	3.0	10.7
	1	0.2	0.5	419.5	496.9	810.2	370.9	439.3	149.3	46.1	34.7	10.8
	1	0.1	0.5	459.4	544.5	887.6	406.2	481.4	74.6	22.9	18.8	23.7
	3	1	1.5	9,931	11,651	894.5	411.6	482.9	2,240	464.5	299.3	25.1
	3	0.6	1.5	12,225	14,187	1,095	506.7	588.0	1,344	200.7	142.7	70.7
	3	0.3	1.5	12,933	15,009	1,158	536.0	622.1	672.0	100.0	78.8	150.2
20% sub-bandgap optical losses	0.4	0.04	0.2	40.0	23.3	559.8	353.7	206.1	11.0	4.7	3.9	5.0
	0.4	0.02	0.2	40.3	24.1	569.0	356.2	212.7	5.5	2.7	2.4	9.1
	1	0.2	0.5	611.7	314.3	818.7	540.8	277.9	137.3	33.5	23.5	9.4
	1	0.1	0.5	668.3	341.9	893.2	590.9	302.3	68.7	16.7	13.0	20.5
	3	1	1.5	15,450	7,019	931.2	640.3	290.9	2,060	310.8	174.8	22.6
	3	0.6	1.5	19,238	7,658	1,115	797.3	317.4	1,236	122.7	77.4	62.4
	3	0.3	1.5	20,252	7,982	1,170	839.4	330.8	617.9	60.7	44.2	131.4

(*) Outer vessel walls are assumed to be 10cm thick in all the cases, R_1 is the inner cylinder radius, L is the cylinder length and R_2 is the outer radius (not considering the vessel walls thickness). (**) total system volume is $\pi L(R_2+0.1)^2$ (***) full-power discharge.

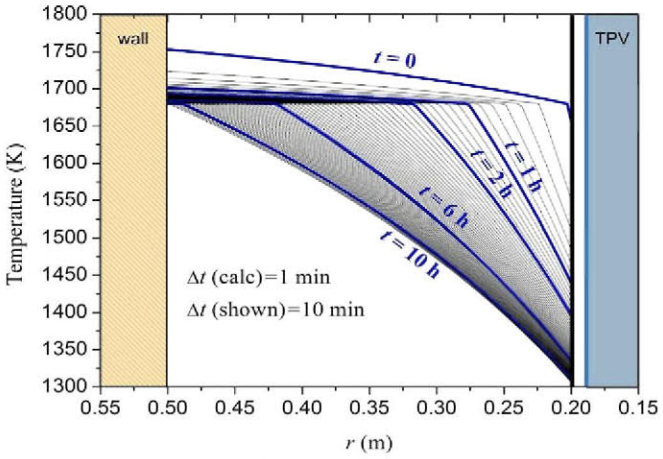

Fig. 6. Temperature profile in the silicon PCM as a function of time for the ES system corresponding to the result shown in Fig.5 (L=1m, R_1=0.2m, R_2=0.5m and ideal 0.5eV TPV cells).

power discharge mode. This peak can be used for power quality applications, such as in uninterruptible power systems (UPS), where high power is required during short periods of time.

Finally, Fig. 6 shows the temperature profile through the PCM (in the radial direction) for the same ES system configuration than in Fig.5. A fast decrease in the emitter temperature (at $r = R_1 = 0.2$ m) is observed during the first instants of operation. This is related to the sharp initial drop in the electrical power shown in Fig.5. This strong drop in the emitter temperature is attributed to the lower Q_s with respect to Q_1 (which is unavoidable because part of Q_1 is employed in performing the phase change), to the decreasing area in the direction of the heat flow (also unavoidable for this particular geometry) and to the lower thermal conductivity of the silicon's solid phase. Notice that the lower emitter temperature, which definitively affects the output electric power, does not necessarily affect the conversion efficiency. This is true at least for ideal TPV converters, for which most of sub-bandgap radiation is reflected back to the emitter. In this case, the lower emitter temperature implies a longer discharging time (due to lower radiative power) instead of lower conversion efficiency.

IV. CONCLUSIONS

A novel ES system utilizing silicon PCM and thermophotovoltaic cells has been presented. This system enables an ultra high energy storage density of ~ 1 MWh/m^3 (heat + electricity) and ~ 500 kWh/m^3 (just electricity). The attractiveness of this concept, besides the extreme energy density, is the use of silicon, the second most abundant element on earth crust.

A theoretical model describing the transient response of the system has been presented. We have used this model to analyze a few different configurations in order to illustrate the system performance.

ACKNOWLEDGEMENT

Authors acknowledge the financial support of the Comunidad de Madrid through the Programme MADRID-PV (Grant number S2013/MAE-2780) and from the Spanish Ministerio de Economía y Competititvidad through the Project PROMESA (grant N. ENE2012-37804-C02-01). C. del Cañizo acknowledges the support of Harvard Real Colegio Complutense through a RCC Fellowship.

REFERENCES

[1] International Energy Agency, "Technology Roadmap: Energy Storage," Mar. 2014.
[2] "marketsandmarkets.com, 2013." .
[3] D. Barlev, R. Vidu, and P. Stroeve, "Innovation in concentrated solar power," *Sol. Enegy Mater. Sol. Cells*, vol. 95, pp. 2703–2725, 2011.
[4] A. Datas, A. Martí, C. del Cañizo, and A. Luque, "Electric energy storage system," 14/198,14.
[5] A. Datas, D. L. Chubb, and A. Veeraragavan, "Steady state analysis of a storage integrated solar thermophotovoltaic (SISTPV) system," *Sol. Energy*, vol. 96, no. 0, pp. 33 – 45, 2013.
[6] D. L. Chubb, B. S. Good, and R. A. Lowe, "Solar thermophotovoltaic (STPV) system with thermal energy storage," 1995, pp. 181–198.
[7] A. Datas, "Optimum semiconductor bandgaps in single junction and multijunction thermophotovoltaic converters," *Sol. Energy Mater. Sol. Cells*, vol. 134, no. 0, pp. 275 – 290, 2015.
[8] A. Veeraragavan, L. Montgomery, and A. Datas, "Night time performance of a storage integrated solar thermophotovoltaic (SISTPV) system," *Sol. Energy*, vol. 108, no. 0, pp. 377–389, Oct. 2014.